ORNL/TM-8355

ornl

OAK
RIDGE
NATIONAL
LABORATORY

UNION
CARBIDE

ORNL/TM--8355

DE83 010407

Neutron and Gamma-Ray Shielding Requirements for a Below-Ground Neutrino Detector System at the Rutherford Laboratory Spallation Neutron Source

T. A. Gabriel
R. A. Lillie
R. L. Childs
J. Wilczynski
B. Zeitnitz

OPERATED BY
UNION CARBIDE CORPORATION
FOR THE UNITED STATES
DEPARTMENT OF ENERGY

ORNL/TM-8355

Contract No. W-7405-eng-26

Engineering Physics Division

Neutron and Gamma-Ray Shielding Requirements for a Below-Ground Neutrino Detector System at the Rutherford Laboratory Spallation Neutron Source

T. A. Gabriel
R. A. Lillie
R. L. Childs*
J. Wilczynski+
B. Zeitnitz+

Date Published - March 1983

*UCC-ND Computer Sciences Division

+Nuclear Research Center,
Karlsruhe, W. Germany

This Work Sponsored by
Office of High Energy & Nuclear Physics
U. S. Department of Energy

OAK RIDGE NATIONAL LABORATORY
Oak Ridge, Tennessee 37830
operated by
UNION CARBIDE CORPORATION
FOR THE
DEPARTMENT OF ENERGY

ABSTRACT

The neutron and gamma-ray shielding requirements for a proposed neutrino detector system below the target station at the Rutherford Laboratory Spallation Neutron Source (SNS) are studied. The present shield below the station consists of 2 meters of iron and 1 meter of concrete, below which is chalk ($CaCO_3$). An underground bunker housing the neutrino detector system would require additional shielding consisting of 6 meters of the chalk plus $\sim$3 meters of iron to reduce the number of high-energy ($\gtrsim$7 MeV) neutrons and gamma rays entering the detector system to an acceptable level of $\sim$1 per day.

INTRODUCTION

The utilization of pulsed neutron spallation sources to carry out low-energy neutrino physics is very appealing due to the relatively large number of neutrinos produced.[1] However, even with very large numbers of produced neutrinos, the interaction rates within multi-ton detector systems are very small, typically on the order of 0.1-10 events/day. To be able to carry out such experiments the background events from all sources must be kept at rates comparable to or less than the rates from incident neutrinos. The purpose of this paper is to define the necessary shielding required to reduce the background event rate from neutrons (and secondary gamma rays) produced at a spallation source, in particular the Rutherford Laboratory Spallation Neutron Source (SNS),[2] to an acceptable level.

When completed, the SNS will utilize 200 μA of 800 MeV protons incident on a fissionable target to produce thermal neutron fluxes comparable to fission reactor fluxes. Since the prime purpose of the SNS is to produce neutrons, little consideration was given to the design of a neutrino experimental area. There are currently two small experimental areas located approximately 2 m underground near the target station. These areas are not adequate for massive neutrino detectors and would be very difficult to shield. Neutrino detectors could be housed aboveground, but due to the large number of neutron experimental areas around the target station the location of the detectors would be situated at distances too large to maintain desirable event rates. In addition, large amounts of shielding would be required. The current proposed location for the detectors is underneath the SNS target station. This is a very desirable

position, not only for shielding neutrons from the spallation source, but also for shielding from galactic sources.

The shielding requirements for a below-ground neutrino detector system will be substantial due to the "small amount" of neutron shielding placed below the target station. Presently, there is only 2 m of iron and 1 m of concrete (assumed to be heavy concrete). Below the concrete is chalk ($CaCO_3$) and it is of relatively low density (2.3×10^3 kg/m^3). To reduce the number of high-energy ($\gtrsim$7 MeV) neutrons and gamma rays entering the detector system to an acceptable level, $\sim$1 per day, will require the building of an underground bunker, the top of which is located 6 m below the concrete base of the target station. Even with the 6 m of chalk above as additional shielding, $\sim$3 m more iron will be required above the detector system. In addition, the concrete walls which will form the bunker must be 1 m thick and have a density of $\gtrsim 3.5 \times 10^3$ kg/m^3.

The tunnel which will provide access to the bunker must be constructed at the bottom of the bunker to prevent loss of shielding around the detector system.

The following sections will describe the one- and two-dimensional calculations carried out to determine the above neutron and gamma-ray shielding requirements.

METHOD OF CALCULATION AND RESULTS

To determine the amount of shielding necessary around the detector system, one-dimensional ANISN[3] and TDA,[4] and two-dimensional DOT[5] transport calculations were carried out. The cylindrical geometry used in the two-dimensional calculations is given in Fig. 1. The spherical geometry

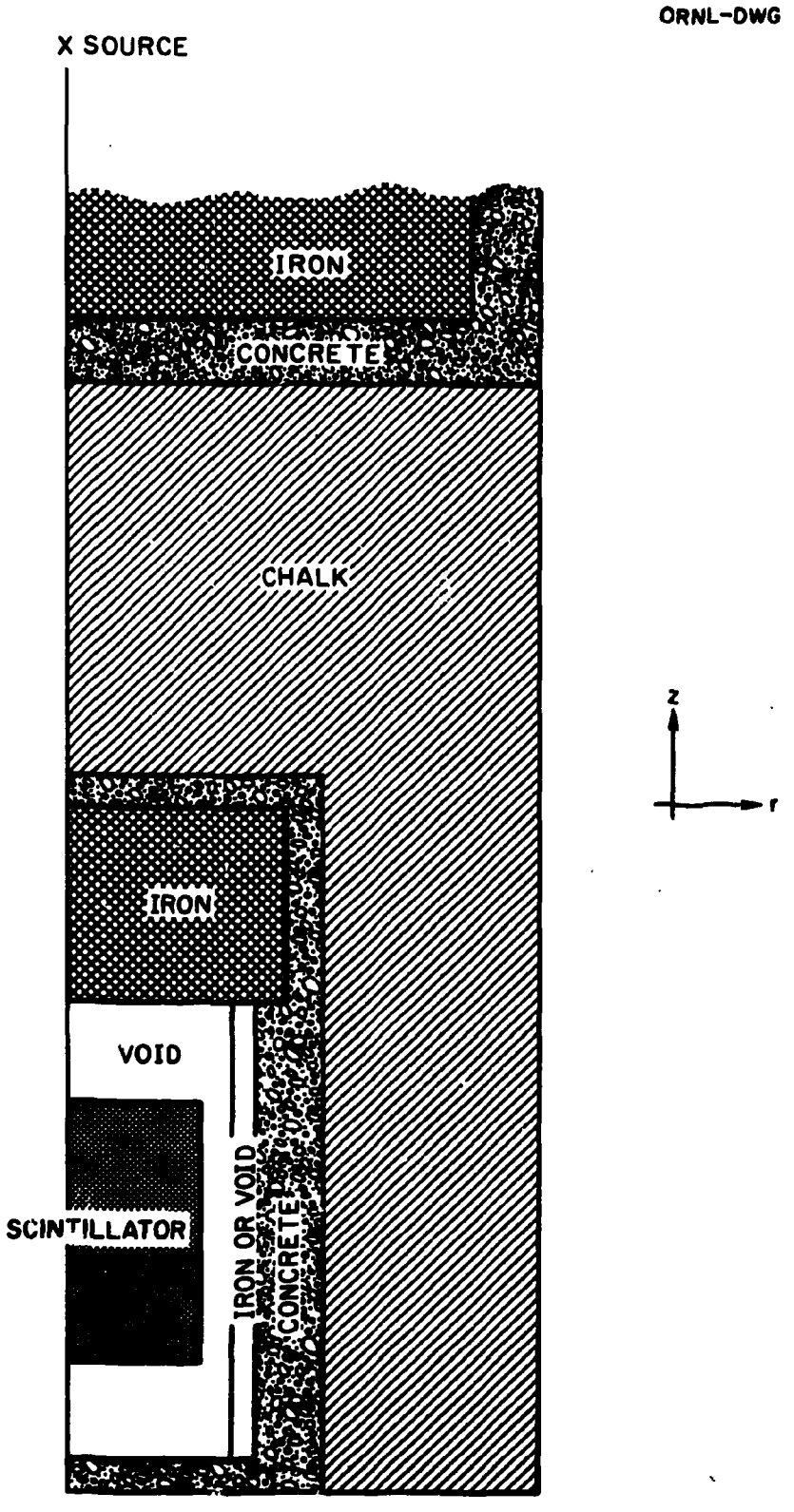

Fig. 1. Two-dimensional geometry for the DOT calculation.

used for the one-dimensional calculations can be obtained from this figure by using the z coordinate to define the radius of each section. The cross sections used for the calculations are given in Ref. 5 and the nuclei density of the materials is given in Table 1.

The neutron spectrum as calculated for 800 MeV protons incident on a Pb target surrounded by a water moderator was used as the neutron source for these calculations. The calculated data have been normalized to 200 μA of 800 MeV protons delivered in a pulse structure of two rectangular pulses (separated by 250 ns from leading edge) of 100 ns duration repeated 50 times/s.

The number of neutrons and gamma rays entering the top of the detector as a function of iron shield thickness is given in Figs. 2 and 3 for no iron shielding inside the bunker and for 0.30 m iron shielding inside the bunker, respectively. The two-dimensional DOT calculations determined the values for 3 m of iron shield thickness and the more cost effective ANISN calculations were used to determine the slopes of the lines and the effectiveness between 5 and 6 m of chalk. The agreement between the one-dimensional ANISN results and the two-dimensional DOT results in Fig. 2 for the 3 m of iron shielding case was generally within 30%. It should be noted that removing the 0.30 m of Fe shielding inside the bunker allows for more streaming to occur around the edge of the large thickness of iron. As can be seen from these figures, ∿3 m of iron is required in addition to the 6 m of chalk to reduce the current of high-energy neutrons (>8.2 MeV) and gamma rays (>5.5 MeV) to below ∿1 per day. It should be remembered that if the surface area of the detector is increased, the number of particles entering the detector

Table 1. Density and Composition of the Materials Used in the Shielding Calculations

Material	Density (g/cm^3)	Nuclei Density (atoms/b·cm)
Fe	7.86	8.49×10^{-2}
Concrete	3.50	
Si		5.31×10^{-4}
Al		1.59×10^{-4}
Fe		2.37×10^{-2}
Ca		1.72×10^{-3}
Mg		9.22×10^{-5}
S		4.63×10^{-5}
C		3.66×10^{-5}
B^{10}		2.24×10^{-3}
B^{11}		6.34×10^{-3}
H		1.04×10^{-2}
O		4.24×10^{-2}
Pb	11.35	3.30×10^{-2}
Scintillator	0.89	
C		4.01×10^{-2}
H		4.87×10^{-2}
Chalk	2.30	
Ca		1.39×10^{-2}
C		1.39×10^{-2}
O_2		4.16×10^{-2}

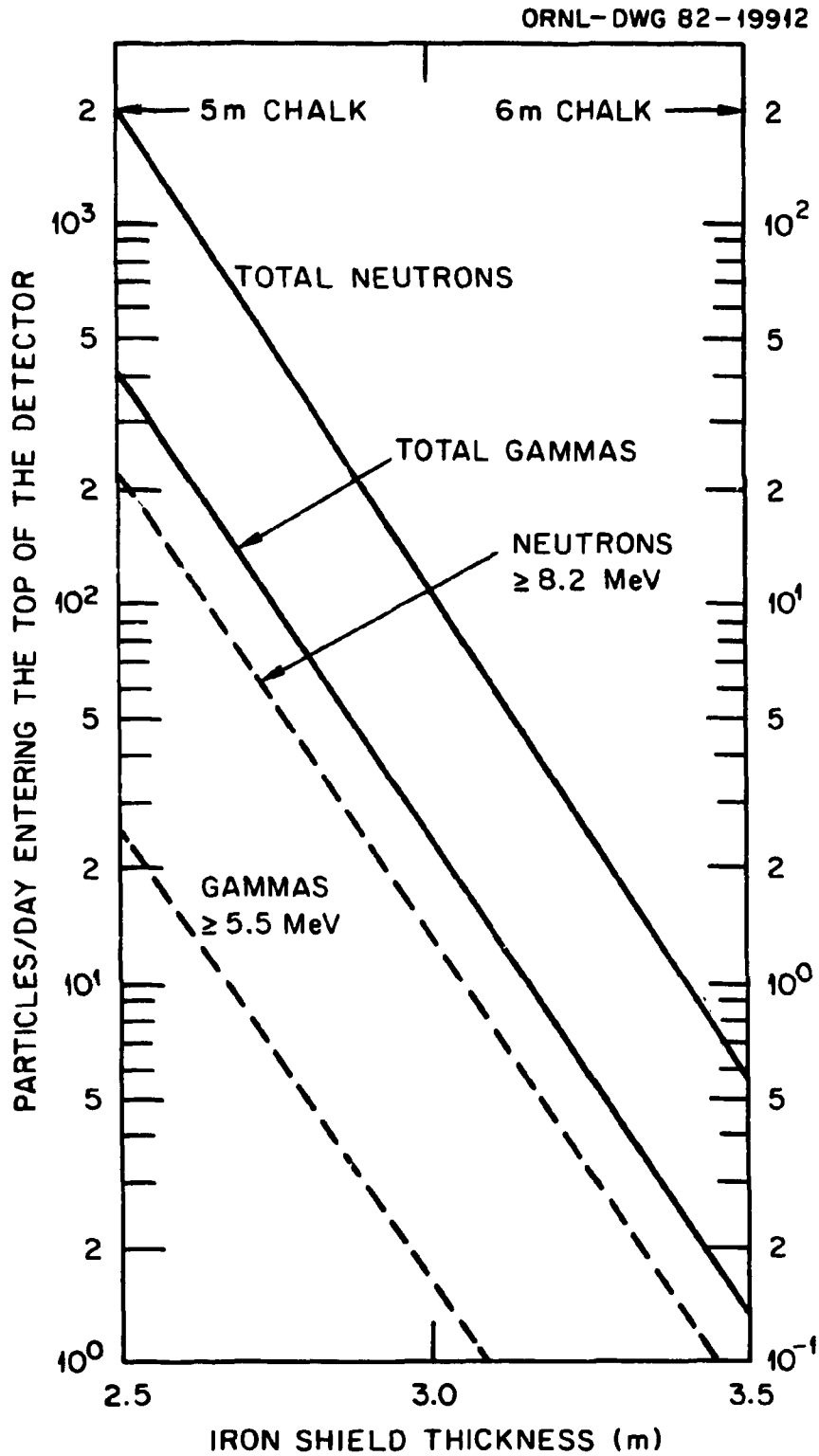

Fig. 2. Particles/day entering the top of the detector as a function of iron shield thickness and chalk thickness (0.0 m Fe shielding inside bunker).

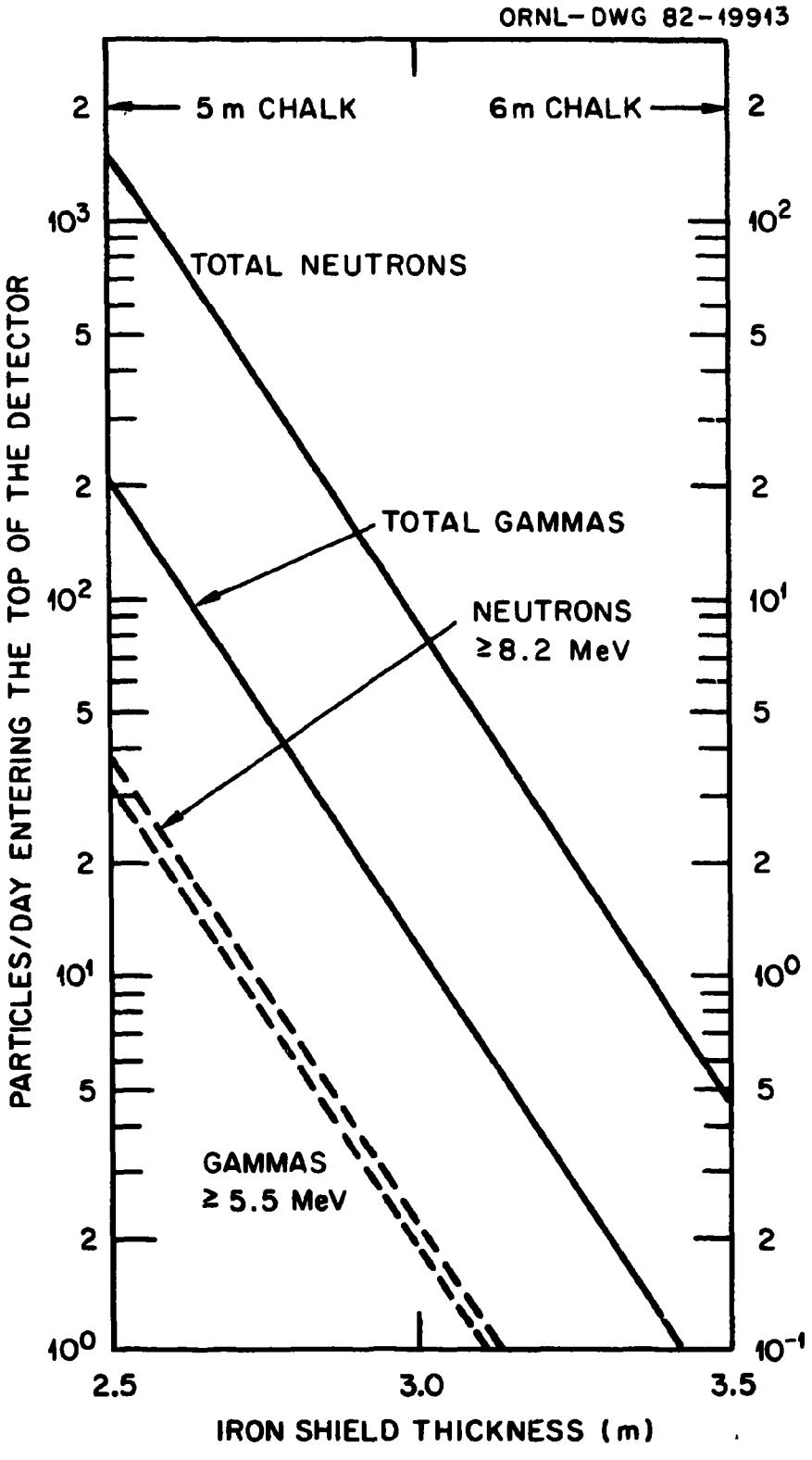

Fig. 3. Particles/day entering the top of the detector as a function of iron shield thickness and chalk thickness (0.30 m Fe shielding inside bunker).

will increase accordingly. The energy dependence of the neutrons and gamma rays entering the detector is presented in Table 2.

There is a safety factor built into these calculations. The actual thickness of iron below the target station is ∿2.4 m (only 2 m has been used in the calculations). However, several streaming paths are located in this structure thereby reducing its effective thickness.

Even though a substantial number of particles enter the detector below ∿7 MeV, they will only contribute to the low-energy background ($\lesssim$10 MeV) and should not interfere with the higher energy signals for ν events, for example, $\nu + e \rightarrow \nu' + e'$ $(E>10\ MeV)^-$ or $\nu + {}^{12}C \rightarrow \nu' + {}^{12}C^*$, ${}^{12}C^* \rightarrow {}^{12}C + \gamma$ $(E = 15\ MeV)$.

The time-dependent structure of the neutron and gamma-ray flux at the top edge of the detector determined from a TDA calculation for 5 m of chalk and 3 m of iron shielding is presented in Figs. 4-7 for various neutron energy ranges and for all gamma energies. Similar data for 6 m of chalk can be obtained from these data by decreasing the results 1 order of magnitude and increasing the time scale by ∿8%. The double peaks in the graphs are the results of the pulse structure of the machine. The high-energy neutrons will come with the pulses of the machine, whereas the thermal neutrons (and somewhat lower energy neutrons) will be much more smeared in time. The pulse structure of the gamma rays will be determined by the neutrons producing them. The two peaks are the results of the fast neutrons while the plateau area for times $\gtrsim 1 \times 10^{-5}$ s is due to thermal neutron captures.

The neutrons and gamma rays that enter the side of the detector must also be considered. The massive amounts of iron and concrete that are

Table 2. Particles/Day Entering Top of Detector as a Function of Fe Thicknesses on Top of and Inside Bunker (6 m Chalk Above Bunker)

Energy Range (MeV)	Particles/Day			
	30 cm Fe Inside Bunker			No Fe Inside Bunker, 3.0 m Fe Top Shield[b]
	2.5 m Fe Top Shield[a]	3.0 m Fe Top Shield[b]	3.5 m Fe Top Shield[a]	
	Neutrons			
∞-275	1.13×10^{-2}	5.47×10^{-4}	2.60×10^{-5}	2.43×10^{-3}
275-160	3.61×10^{-2}	1.93×10^{-2}	1.03×10^{-3}	9.69×10^{-2}
160-90	1.33×10^{0}	7.37×10^{-2}	4.03×10^{-3}	4.29×10^{-1}
90-55	1.04×10^{0}	5.77×10^{-2}	3.15×10^{-3}	3.51×10^{-1}
55-30	7.34×10^{-1}	4.03×10^{-2}	2.21×10^{-3}	2.29×10^{-1}
30-17.5	3.42×10^{-1}	2.56×10^{-2}	1.03×10^{-3}	1.29×10^{-1}
17.5-8.18	4.30×10^{-1}	2.37×10^{-2}	1.29×10^{-3}	1.20×10^{-1}
8.18-3.01	9.16×10^{-1}	5.03×10^{-2}	2.74×10^{-3}	2.45×10^{-1}
3.01-1.10	3.26×10^{0}	1.79×10^{-1}	9.77×10^{-3}	5.48×10^{-1}
$1.10-2.24\times10^{-1}$	3.36×10^{1}	1.86×10^{0}	1.02×10^{-1}	2.36×10^{0}
$2.24\times10^{-1}-7.10\times10^{-3}$	5.19×10^{1}	2.88×10^{0}	1.58×10^{-1}	3.22×10^{0}
$7.10\times10^{-3}-2.26\times10^{-5}$	4.33×10^{1}	2.41×10^{0}	1.33×10^{-1}	2.49×10^{0}
$2.26\times10^{-5}-4.14\times10^{-7}$	9.28×10^{0}	5.15×10^{-1}	2.84×10^{-2}	5.19×10^{-1}
4.14×10^{-7}-0	3.60×10^{0}	2.00×10^{-1}	1.09×10^{-2}	1.18×10^{-1}
	Gamma Rays			
∞-7.5	2.08×10^{0}	1.15×10^{-1}	6.31×10^{-3}	9.57×10^{-2}
7.5-5.5	1.06×10^{0}	5.86×10^{-2}	3.22×10^{-3}	6.23×10^{-2}
5.5-3.5	1.10×10^{0}	6.08×10^{-2}	3.33×10^{-3}	7.62×10^{-2}
3.5-1.5	2.51×10^{0}	1.39×10^{-1}	7.62×10^{-3}	1.98×10^{-1}
1.5-0.01	1.42×10^{1}	7.85×10^{-1}	4.31×10^{-2}	1.95×10^{0}

[a]Scaled from ANISN calculations.

[b]From DOT calculations.

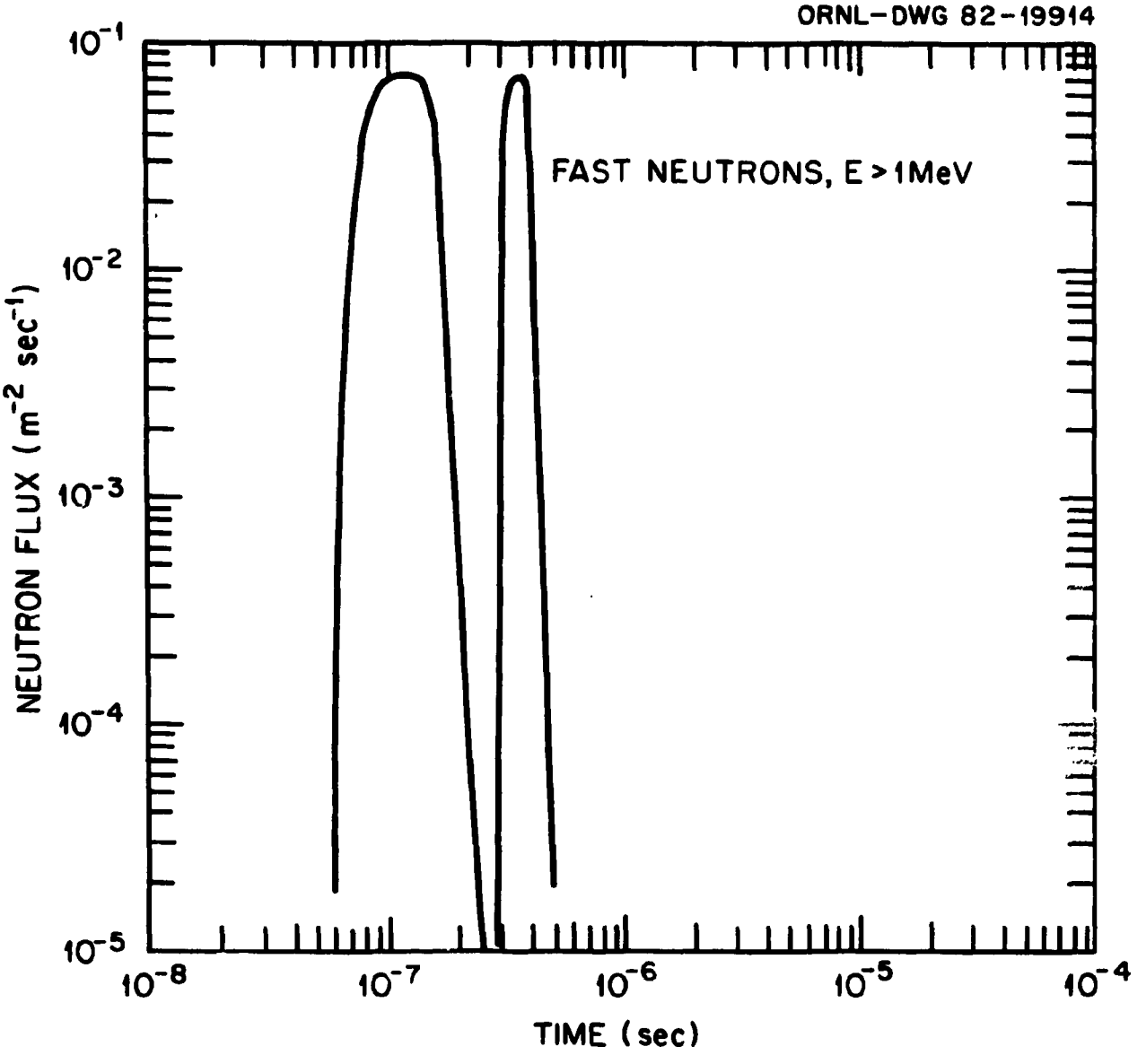

Fig. 4. Time-dependence of the fast neutron flux at the top edge of the detector.

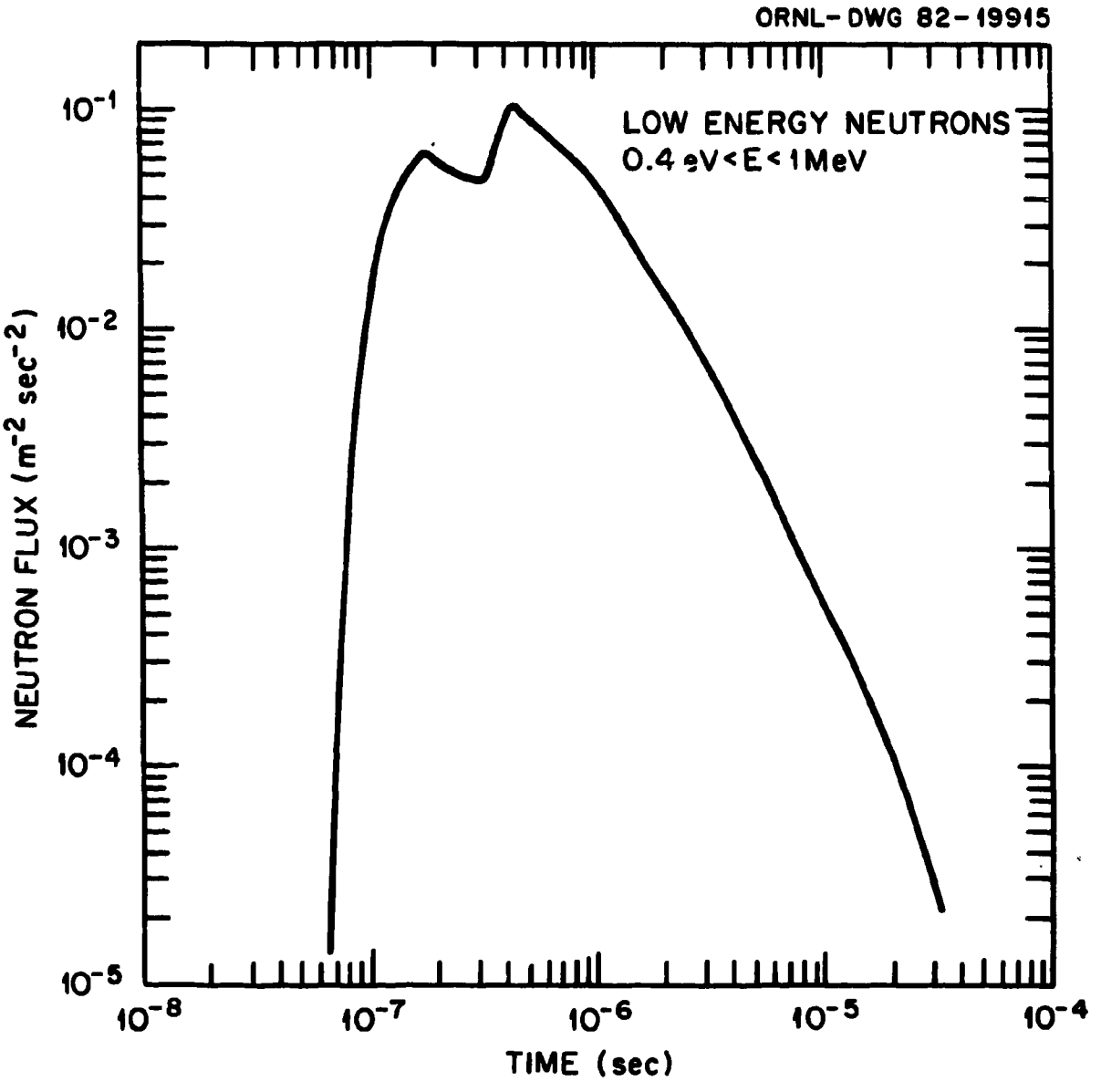

Fig. 5. Time-dependence of the low-energy neutron flux at the top edge of the detector.

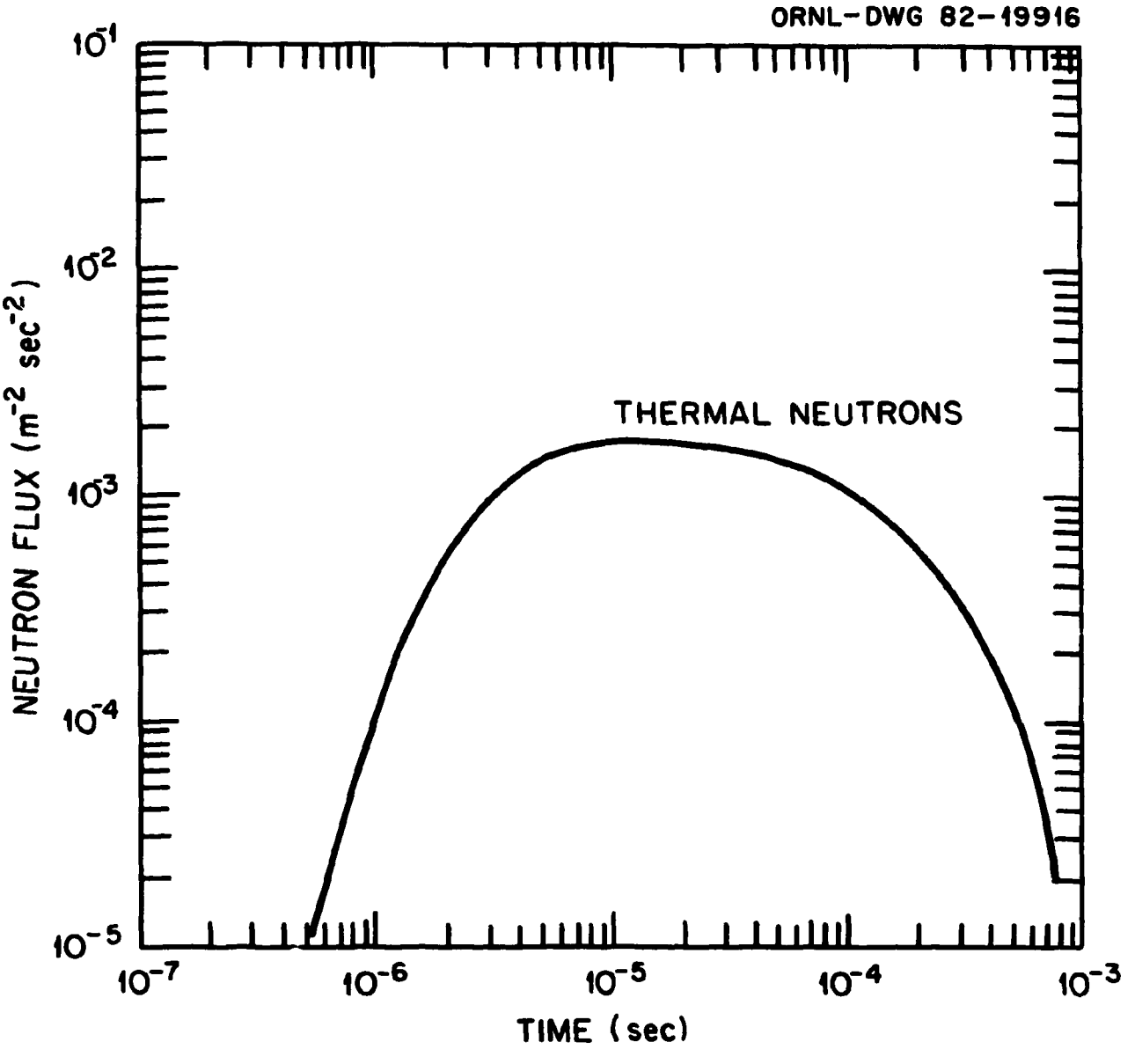

Fig. 6. Time-dependence of the thermal neutron flux at the top edge of the detector.

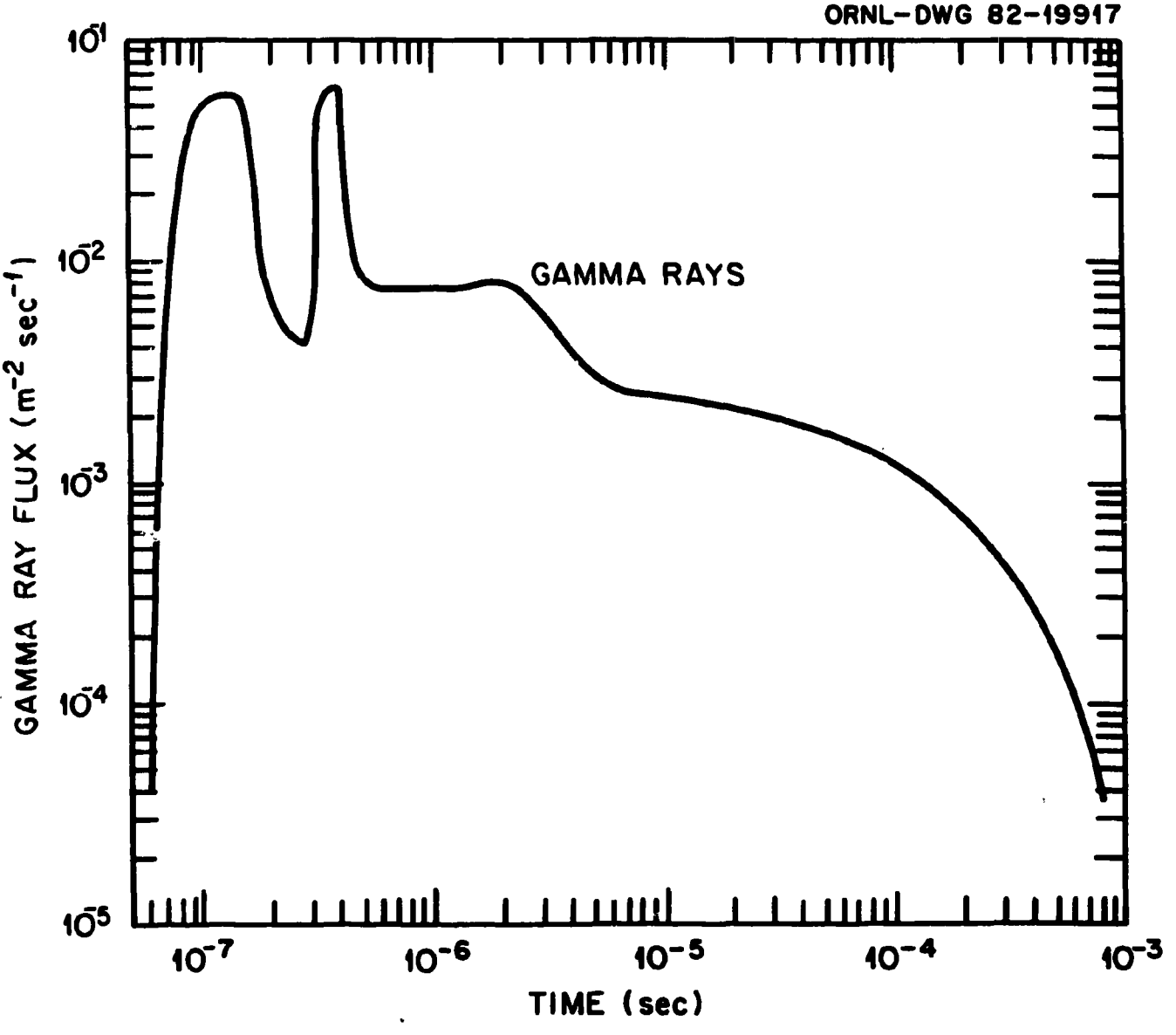

Fig. 7. Time dependence of the gamma-ray flux at the front edge of the detector.

above the detector can shadow shield many neutrons and gamma rays approaching the detector. However, neutrons are not very well attenuated by chalk. For example, whereas 1 m of iron attenuates neutrons by a factor of ∿300 and 1 m of heavy concrete by a factor of ∿100, 1 m of chalk attenuates by a factor of only ∿10. Neutrons which come down the side of the bunker in the chalk can scatter to the side and enter the detector room through the heavy concrete. The results of calculations to determine the leakage of particles into the side of the detector are presented in Figs. 8-10 and Table 3.

As before the results of the two-dimensional calculations have been used to determine the data points for 0 and 0.30 m iron shield thicknesses inside the bunker and more approximate ANISN slab calculations have been used to determine the slopes. The source term for the ANISN slab calculation was obtained from an ANISN spherical calculation by considering the current of particles which can enter the concrete from the chalk regions. The curves in Fig. 8, therefore, must be considered as very approximate.

The buildup in the total number of neutrons as indicated in Fig. 8 is the direct result of a re-buildup of low energy and thermal neutrons from high energy (n,2n), (n,3n), (n,4n), etc. reactions. The boron in the concrete kept the thermal neutrons at a low level. The buildup of the gammas $\geq$5.5 MeV is a direct result of the thermal neutron buildup.

As can be seen, the shielding requirements are substantial to reduce the background from the neutrons originating at the SNS source to an acceptable level. These calculations have not taken into account any stacking problems of the iron shielding which can lead to streaming paths.

The area which will be most affected by this is the Fe-concrete interface. Gaps in this area can lead to substantial increases in

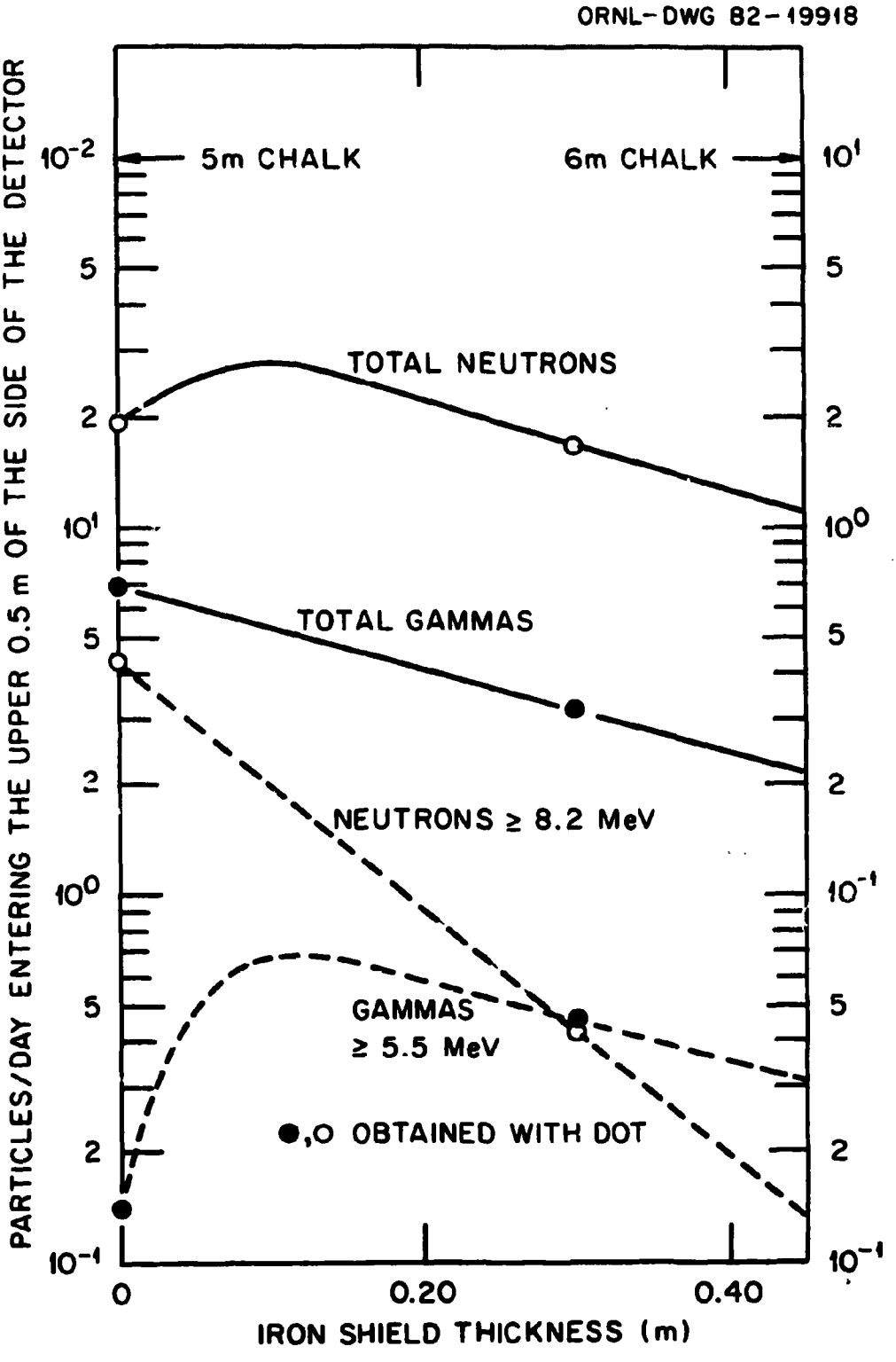

Fig. 8. Particles/day entering the upper 0.50 m of the side of the detector for 3 m of top Fe shielding as a function of Fe shield thickness inside of bunker.

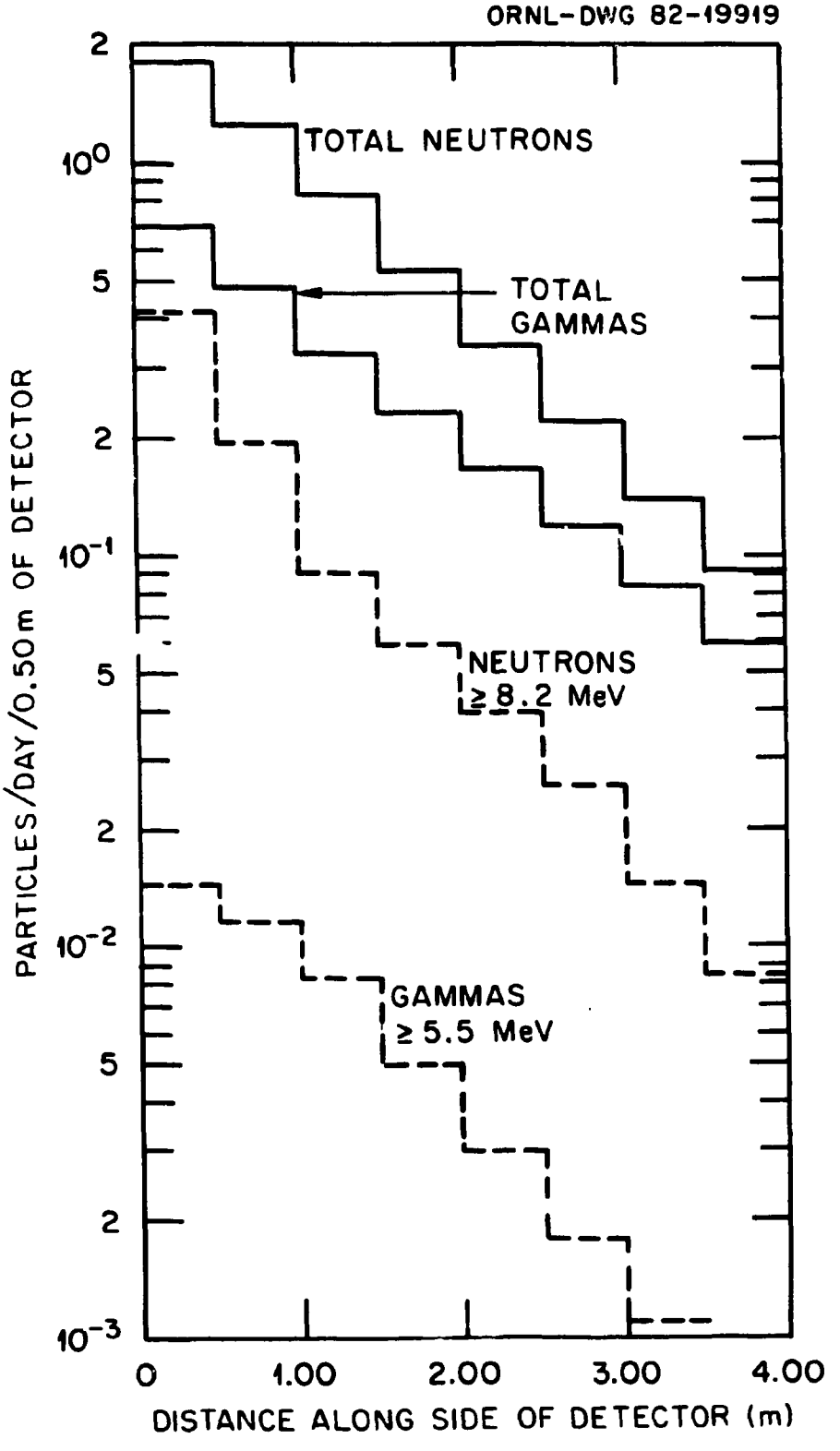

Fig. 9. Particles/day entering the side of the detector for 3 m of top Fe shielding and 0.0 m of Fe shielding inside of bunker (6 m chalk).

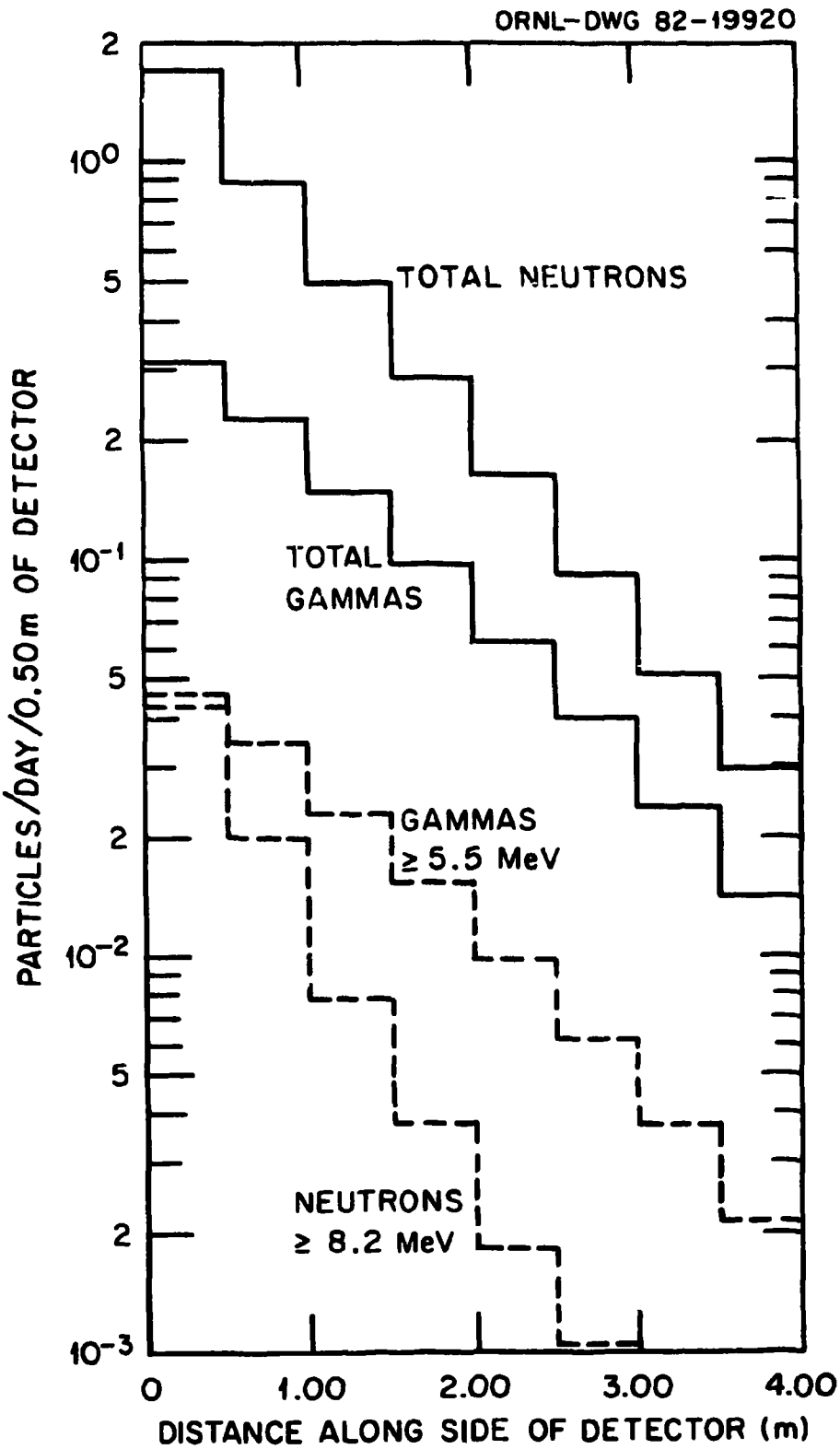

Fig. 10. Particles/day entering the side of the detector for 3 m of top Fe shielding and 0.30 m of Fe shielding inside the bunker (6 m chalk).

Table 3. Particles/Day Entering Upper 50 cm of the Side of the Detector for a 3-meter Top Fe Shield and Two Fe Shield Thicknesses Inside Bunker (6 m Chalk Above Bunker)

Energy Range (MeV)	Particles/Day	
	No Fe Inside Bunker	30 cm Fe Inside Bunker
	Neutrons	
∞-275	1.27×10^{-3}	8.06×10^{-5}
275-160	4.25×10^{-2}	3.10×10^{-3}
160-90	1.50×10^{-1}	1.28×10^{-2}
90-55	1.01×10^{-1}	1.02×10^{-2}
55-30	6.09×10^{-2}	7.38×10^{-3}
30-17.5	3.45×10^{-2}	4.84×10^{-3}
17.5-8.18	3.47×10^{-2}	4.66×10^{-3}
8.18-3.01	7.56×10^{-2}	1.14×10^{-2}
3.01-1.10	1.41×10^{-1}	4.46×10^{-2}
$1.10-2.24\times10^{-1}$	3.55×10^{-1}	4.02×10^{-1}
$2.24\times10^{-1}-7.10\times10^{-3}$	4.64×10^{-1}	5.75×10^{-1}
$7.10\times10^{-3}-2.26\times10^{-5}$	3.56×10^{-1}	4.46×10^{-1}
$2.26\times10^{-5}-4.14\times10^{-7}$	3.74×10^{-2}	1.29×10^{-1}
4.14×10^{-7}-0	1.56×10^{-3}	5.82×10^{-2}
	Gamma Rays	
∞-7.5	6.75×10^{-3}	3.09×10^{-2}
7.5-5.5	7.68×10^{-3}	4.63×10^{-2}
5.5-3.5	1.16×10^{-2}	6.23×10^{-2}
3.5-1.5	3.41×10^{-2}	9.88×10^{-2}
1.5-0.01	6.34×10^{-1}	3.18×10^{-1}

background rates. Even though no additional iron shielding appears necessary along the side of the walls inside the bunker, the stacking problems will probably dictate additional localized shielding around the top of the bunker area.

REFERENCES

1. B. Zeitnitz, "Neutrino Physics at the Spallation Neutron Source," KFK 3155 (March, 1981), also KFK 3174 (June, 1981).
2. F. Atchison, "A Theoretical Study of a Target Reflector and Moderator Assembly for SNS," RL81-006, SNS/TRAM/P5/80 revised, Rutherford Laboratory (April, 1981).
3. W. W. Engle, Jr., "A Users Manual for ANISN," K-1693, Oak Ridge National Laboratory (1967).
4. S. A. Dupree et al., "Time-Dependent Neutron and Photon Transport Calculations Using the Method of Discrete Ordinates," ORNL-4662, Oak Ridge National Laboratory (1971).
5. W. A. Rhoades and F. R. Mynatt, "The DOT III Two-Dimensional Discrete Ordinates Transport Code," ORNL/TM-4280, Oak Ridge National Laboratory (1973).
6. R. G. Alsmiller, Jr. and J. Barish, "Neutron-Photon Multigroup Cross Sections for Neutron Energies $\leq$400 MeV," ORNL/TM-7818, Oak Ridge National Laboratory (1981).

ORNL/TM-8355

Internal Distribution

1. L. S. Abbott
2. F. S. Alsmiller
3. R. G. Alsmiller, Jr.
4. D. E. Bartine
5. B. L. Bishop
6. A. A. Brooks
7-9. R. L. Childs
10. G. F. Flanagan
11-15. T. A. Gabriel
16-20. EPD Reports Office
21-23. R. A. Lillie
24. F. C. Maienschein
25. B. F. Maskewitz
26. R. W. Peelle
27. R. T. Santoro
28. C. R. Weisbin
29. R. M. Westfall
30. A. Zucker
31. P. W. Dickson, Jr. (Consultant)
32. H. J. C. Kouts (Consultant)
33. W. B. Loewenstein (Consultant)
34. R. Wilson (Consultant)
35. Central Research Library
36. Document Reference Section
37. ORNL Y-12 Technical Library Document Reference Section
38-39. Laboratory Records Department
40. Laboratory Records, RC
41. ORNL Patent Office

External Distribution

42. Office of Assistant Manager for Energy Research and Development, DOE-ORO, Oak Ridge, TN 37830
43. Dr. R. Eisenstein, Department of Physics, University of Illinois, Urbana, IL 61801
44. Dr. E. Fowler, Department of Physics, Purdue University, West Lafayette, IN 47907
45. Dr. G. T. Gillies, Department of Physics, University of Virginia, Charlottesville, VA 22901
46. Dr. M. Goodman, Department of Physics, Harvard University, Cambridge, MA 02138
47. Dr. J. LoSecco, Department of Physics, California Institute of Technology, Pasadena, CA 91125
48. Dr. V. S. Narasimham, Tata Institute of Fundamental Research, Bombay 400 005, India
49. Dr. F. Nezrick, Division of High Energy and Nuclear Physics, Department of Energy, Washington, D.C. 20545
50. Dr. T. R. Palfrey, Jr., Department of Physics, Purdue University, West Lafayette, IN 47907
51. Dr. C. Rubbia, Lyman Laboratory, Harvard University, Cambridge, MA 02138
52. Dr. M. Shupe, Department of Physics, University of Minnesota, Minneapolis, MN 55455
53. Dr. L. Sulak, Department of Physics, University of Michigan, Ann Arbor, MI 48109
54. Dr. D. Winn, Lyman Laboratory, Harvard University, Cambridge, MA 02138
55. Dr. W. A. Wallenmeyer, Division of High Energy and Nuclear Physics, Department of Energy, Washington, D.C. 20545

External Distribution (Cont'd)

56-57. Dr. J. Wilcznski, Nuclear Research Center, Karlsruhe, W. Germany
58-59. Dr. B. Zeitnitz, Nuclear Research Center, Karlsruhe, W Germany
60-86. Technical Information Center (TIC)
87-133. Given High-Energy Accelerator Shielding distribution

Printed in the United States of America. Available from
National Technical Information Service
U.S. Department of Commerce
5285 Port Royal Road, Springfield, Virginia 22161
NTIS price codes—Printed Copy: A03; Microfiche A01